FUDMA Journal of Sciences (FJS)
ISSN online: 2616-1370
ISSN print: 2645 - 2944
Vol. 10 No. 1, January, 2026, pp 1 – 14
DOI: https://doi.org/10.33003/fjs-2026-1001-4116

URBAN GROWTH AND THERMAL ENVIRONMENT DYNAMICS IN KADUNA, NIGERIA: LAND USE CHANGE, UHI, UTFVI, AND A NOVEL VEGETATION COOLING EFFICIENCY INDEX

***Habiba Ibrahim Mohammed and Maryam Mustapha**

Department of Geography and Sustainability Studies, Kaduna State University, Kaduna, Nigeria.

*Corresponding authors' email: mydearhabiba@yahoo.com

ABSTRACT

Rapid urbanization has accelerated land use/land cover (LULC) changes and accompanying thermal stress in cities across sub-Saharan Africa. This study investigated the relationships between urban growth and ecological thermal conditions in Kaduna Metropolis, Nigeria, between 2004 and 2024 via Landsat data and remote sensing indices. LULC was divided into five classes—bare terrain, built-up areas, cultivated lands, tree cover, and water bodies—through multiresolution segmentation and a decision tree algorithm. The land surface temperature (LST) was derived via thermal bands, whereas the urban heat island (UHI) intensity and the urban thermal field variance index (UTFVI) were employed to measure spatial changes in thermal stress. This study introduces the Vegetation Cooling Efficiency Index (VCEI) to evaluate the cooling impact of vegetation. The results demonstrate strong increases in built-up areas (+121.04 km²) and bare fields (+596.19 km²), mostly at the expense of cultivated lands (–525.54 km²) and tree cover (–191.91 km²). The mean LST rose from 32.2 °C in 2004 to 35.7 °C in 2024, with significant geographic differences in surface heating. UHI hotspots persisted in urban cores; however, the maximum intensity decreased significantly (from +5.27 °C to +3.72 °C), whereas the UTFVI suggested moderate and rather stable ecological thermal stress. The VCEI confirmed the continuous cooling effect of vegetation, while its efficacy diminished with vegetation removal. These findings reinforce the importance of unplanned urban growth in modifying thermal settings and highlight the necessity of green infrastructure and vegetation preservation in promoting ecological resilience and thermal comfort.

Keywords: Urban growth, Land surface temperature, Urban heat island, UTFVI, VCEI, Kaduna metropolis

INTRODUCTION

Owing to rapid population growth, infrastructure development, and industrialization, urbanization has become a global environmental issue (Amir Siddique et al., 2024). The world's urban population is projected to increase by 2.5 billion between 2018 and 2050, with approximately 90% of this increase occurring in Africa and Asia (Sharma & Vashishtha, 2024). Nigeria is among the most urbanized regions in sub-Saharan Africa, with an annual rate of urbanization of 3.5% (World Bank, 2024). According to Statista (2024), the share of Nigeria's urban population rose to 53.52 percent in the year 2022. Kaduna metropolis, particularly, has experienced tremendous growth in population, from approximately 250,000 in the 1960s to over three (3) million people in the year 2024 (Kaduna Bureau of Statistics, 2024). This increase in urbanization has led to the modification of land cover across the globe, significantly impacting humans and causing severe environmental degradation (Rashid et al., 2022).

Changes in land use and land cover have been identified as key factors influencing land surface temperature (LST) (Al Shawabkeh et al., 2024), although previous studies have reported that LST is influenced by a combination of other factors, such as the removal of vegetation (Abubakar et al., 2024), physical properties of construction materials, buildings, morphology, surface roughness (Litardo et al., 2020; Tesfamariam et al., 2024), and anthropogenic heat sources. These changes impact the thermal capacity of cities, heat conductivity, and albedo coefficient (Kusumawardani & Hidayati, 2022). The Intergovernmental Panel on Climate Change (IPCC) projects that atmospheric carbon dioxide levels will double from preindustrial levels by 2100 and that the average global land surface temperature (LST) will rise by 1.4–5.8 °C (Faisal et al., 2021). Furthermore, this uncontrolled increase in LST has been identified as the main driver of the formation of the urban heat island (UHI) effect globally (Das et al., 2020; Koko, Yue, et al., 2021). The UHI effect is defined as the difference in air and surface temperatures between urban centers and their natural surroundings (Hidalgo-García & Arco-Díaz, 2022; Koko, Wu, et al., 2021; Ullah et al., 2024), and it has become a serious concern to researchers because of its negative impact on human health (Muhammad & Abubakar, 2025), as well as environmental variables such as air quality, precipitation, temperature, carbon storage, and energy balance (Rousta et al., 2018). Additionally, increased energy consumption in cities as a result of warming can significantly impact SDG-3 to ensure healthy lives and promote well-being at all ages (Ünsal et al., 2024), SDG-6 for clean and affordable energy (Mahato et al., 2024), SDG-11 for sustainable cities and communities, and SDG-13 climate action (Ünsal et al., 2024). Thus, studying thermal islands is critical in regional planning (Zandi et al., 2022).

Remote sensing provides adequate spatial and spectral resources that can be used to study urban-related issues at the macro level (Abubakar, 2019). Moreover, freely available sensors from Landsat, Moderate Resolution Imaging Spectroradiometer (MODIS), and Sentinel satellites/sensors have provided multispectral and multitemporal images that have been used in urban studies (Adão et al., 2024; Amir Siddique et al., 2024; Andronis et al., 2022; Arias et al., 2024; Naserikia et al., 2024; Peng et al., 2020; Sandoval et al., 2024; Shukla & Jain, 2021; Singh et al., 2024; Sugianto et al., 2024; Taripanah & Ranjbar, 2021). Specifically, studies have applied UHIs and UTFVIs to study thermal comfort in cities globally (Mhana et al., 2024; Moisa & Gemeda, 2022; Patel et al., 2024; Rao et al., 2024; Rashid et al., 2022; Siswanto et al., 2024; Tesfamariam et al., 2024; Wemegah et al., 2020; Zandi et al., 2022).

In the Kaduna metropolis, different studies have been carried out on land surface temperature. For example, Zaharaddeen et al. (2016) estimated the LST in the Kaduna Metropolis via Landsat images and reported a negative relationship between

the vegetation density and land surface temperature. Abubakar et al. (2024) assessed the relationship between the LST and NDVI via MODIS time series data. However, on the basis of the available literature, studies on surface urban heat island intensity (SUHII) and the urban thermal field variance index (UTFVI) are rare.

In recent years, the Kaduna metropolis has experienced a significant expansion of settlements due to rapid population growth (Amin & Dadan-Garba, 2014). According to records from Nigeria's National Bureau of Statistics (http://www.citypopulation.de/), the population of the Kaduna metropolis increased from approximately 993,642 in 1991 to 1.9 million by 2022. Additionally, the city witnessed infrastructural development, construction and upgrades of existing road networks, and construction of neighborhood centers, among others, as part of the Urban Renewal Programme (Kaduna State Government, 2021). This has led to an increase in impervious surfaces and the removal of vegetation, which intensifies urban heat islands.

Previous studies in Kaduna have examined the LST and NDVI, but little is known about the SUHII and UTFVI, and no study has quantified the cooling efficiency of vegetation. Thus, this study aimed to assess the changes in land use, vegetation, and surface temperature and their relationships with the UHI and UTFVI phenomena via remote sensing. This study also proposes the vegetation cooling efficiency index (VCEI) on the basis of the relationship between surface temperature and vegetation. Finally, the findings from this study can help policymakers and urban planners plan for a sustainable environment in the future.

MATERIALS AND METHODS

Study Area

The Kaduna Metropolis is composed of the Kaduna North and Kaduna South Local Government Areas and parts of the Chikun and Igabi Local Government Areas (Akpu et al., 2017). The Kaduna Metropolis lies between latitudes 10°20′00″ and 10°39′00″ North of the Equator and between longitudes 7°20′16″ and 7°35′00″ East of the Greenwich Meridian, with an area of 3156 km^2 (see Figure 1). The metropolis is bordered from the north, northeast, and northwest by the rest of the Igabi Local Government Area and from the south, southeast, and southwest by the rest of the Chikun Local Government Area (Baba et al., 2020).

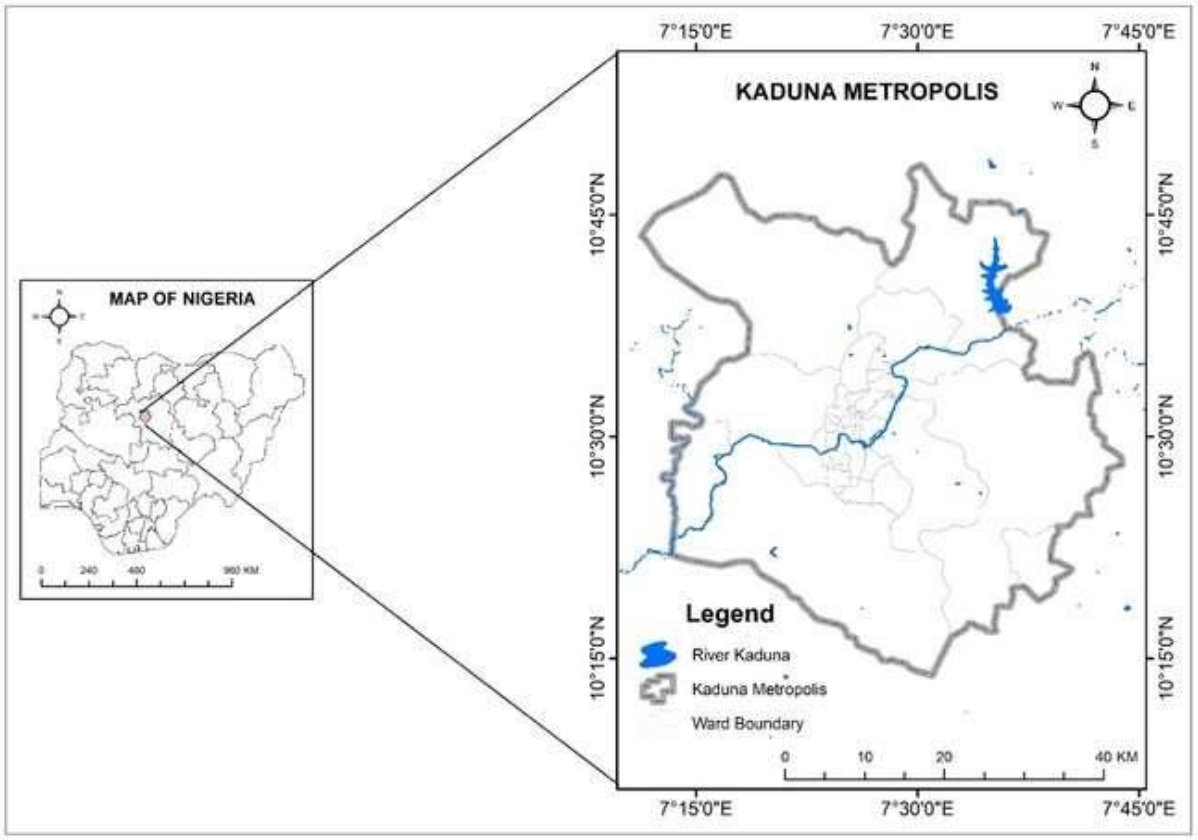

Figure 1: The study area showing the elevation of the Kaduna metropolis
Source: GRID3 - Nigeria, (2022)

Kaduna is situated in a tropical wet and dry climate (Abdussalam, 2020). The wet season runs for approximately six to seven months, mostly between April and October, with an average rainfall of 1400 mm. The dry season denotes Harmattan, which has severe dust haze, with northerly winds blowing from the desert (Abubakar & Abdussalam, 2024). The maximum temperature in Kaduna metropolis can be over 30 °C, with the hottest months being March, April and May. The relative humidity typically ranges from 25% to 90% depending on the month of the year, with the lowest humidity occurring between December and February (Ahmed et al., 2024).

The relief of Kaduna as a plain, comprising extensive tracts of almost level to gently undulating, lightly dissected land, is broken in places by groups of rocky hills and inselbergs. Much of the area lies between 600 and 800 m, with scattered hills rising 50–200 m above the surrounding land (Bennett et al., 1979). The drainage net is predominantly tributary to the Niger via the Kaduna and Gurara Rivers. Downcutting by rivers is most common in the southern and western margins

of the Kaduna Plains (Musa & Abubakar, 2024). The area lies in the northern Guinea savannah zone. Therefore, it has a savanna grassland type of vegetation that is made up of tall grasses, scattered trees, and a gallery. Fringe forests, "*Kurmi*" in Hausa in some localities, are presently at the mercy of increasing demands for fuel wood in fast-growing towns and urban centers (Ajibade & Okwori, 2009).

Data used

Three Landsat satellite images, ETM+ from 2004 and OLI/TIRS from 2014 and 2024, were obtained from the USGS website. The cloud coverage of both datasets was less than 10%. These Landsat images (Table 1) were obtained to analyze the LULC and LST in Kaduna; hence, the date was chosen to be between December and February to prevent foggy pixel difficulties. To perform spatial analysis, all of these datasets were transformed to a 30 m cell size and combined into a single projection. All satellite photos were preprocessed, and the necessary activities for LULC classification and LST computation were carried out in ArcGIS 10.8.

Table 1: Characteristics of the Landsat images used

Sensor	Path	Row	Date of Acquisition
Landsat 7 (ETM+)	189	053	2004/03/04
Landsat 8 (OLI/TIRS)	189	053	2014/12/20
Landsat 8 (OLI/TIRS)	189	053	2024/02/15

Method

Image classification

The decision tree/CART algorithm on Trimble eCognition was used to classify land use into five major classes. The land use classes are bare land, built-up areas, cultivated land, tree cover, and water bodies (Table 2). Decision tree/CART was used because it is highly reliable and is suitable for index-based classification (Laliberte et al., 2007; Phiri et al., 2020).

Table 2: Land cover categories

Land Use Class	Description
Bare land	Exposed soil layer, landfills, and excavated areas
Built Areas	Residential, institutional, industrial, roads, rail, etc.
Cultivated Lands	Cultivated areas, croplands, and grasslands.
Tree Cover	Natural (undisturbed) vegetation.
Water Bodies	Rivers, streams, lakes, and reservoirs.

For this study, two steps were involved in the classification. The first stage was multiresolution segmentation, where the images were broken into objects. A threshold was subsequently employed to determine a class via ranges from computed remote sensing indices. The classification was subsequently carried out via decision trees. This approach is one of the most instinctive classifiers, using decision rules that convert inputs such as indices or spectral reflectance into discrete themes as outputs or LULC classes (Agarwal & Sharma, 2011). Furthermore, decision trees that have more than one input are important for classification. For example, spectral reflectances from Landsat and elevation data are incorporated into the classification scheme (Kodors, 2019).

Accuracy assessment

To determine the proportion of correctly identified pixels, an accuracy evaluation was carried out to compare the LULC classifications. Both kappa statistics and overall accuracy (Congalton, 1991) were calculated for this purpose. Accuracy assessment is an unavoidable step in LULC mapping, as the increased complexity of classification increases the chance of error (Bharath et al., 2020; Congalton, 1991; Rwanga & Ndambuki, 2017). One of the major challenges of this process is the availability of maps used to examine the validity of image analysis (Basu & Das, 2021). For this study, we used high-resolution imagery (Google Earth imagery from the HCMGIS plugin and orthophotography). In this approach, we used historical images to validate land use and land cover maps of the same periods. Points are taken randomly for accuracy assessment (Alawamy et al., 2020).

The error matrix from the accuracy assessment is used to compare the polygon or pixel of the classification result to the real-world (ground-truth) data (Peacock, 2014). These matrices mirror the overall accuracy and the Kappa coefficient value for each year. An overall accuracy greater than 70% is generally considered acceptable, and a kappa coefficient between 0.40 and 0.85 indicates good correspondence (Congalton, 1991).

The kappa coefficient is calculated via Eq. (1):

$$Kappa = \frac{Observed\ accuracy - Expected\ accuracy}{1 - Expected\ accuracy} \quad (1)$$

LST Retrieval

To compute the LST, the Landsat spectral data were converted to radiance. The formula is given below:

Conversion of DN values to spectral radiance

The satellite data products were a geometrically corrected dataset. The first step of the proposed work is to convert the digital number (DN) values of band 10 to at-sensor spectral radiance via Eq. (2).

$$L\pi = \frac{(L_{max} - L_{min}) * Q_{cal}}{(Q_{calmax} - Q_{calmin})} + L_{min} - O_i \quad (2)$$

where L_{max} is the maximum radiance ($Wm^{-2}sr^{-1}\mu m^{-1}$), L_{min} is the minimum radiance ($Wm^{-2}sr^{-1}\mu m^{-1}$), Q_{cal} is the DN value of the pixel, $Q_{cal\ max}$ is the maximum DN value of the pixels, $Q_{cal\ min}$ is the minimum DN value of the pixels, and O_i is the correction value for band 10.

After the DN values are converted to at-sensor spectral radiance, the TIRS band data are converted to brightness temperature (BT) via Eq. (3):

$$BT = \frac{K2}{ln\left[\left(\frac{K1}{L_\pi}\right)\right] + 1} - 273.15 \quad (3)$$

where K1 and K2 are the thermal constants of TIR band 10 and can be identified in the metadata file associated with the satellite image (Avdan & Jovanovska, 2016; Barsi, Lee, et al., 2014; Barsi, Schott, et al., 2014). To obtain results in degrees Celsius, it is necessary to revise by adding absolute zero, which is approximately equal to -273.15 °C. Since the

atmosphere in our research area is relatively dry and therefore, the range of water vapor values is relatively small, the atmospheric effect is not taken into consideration when retrieving the LST.

The LSE calculation is required to estimate the LST.

The LSE is defined as the ratio of the radiance emitted by an object to the radiance it would emit if it were a perfect black body at the same thermodynamic temperature (Norman & Becker, 1995). Extensive measurements of LSE have been made because of its importance to satellite remote sensing of LST (Becker, 1987), surface energy balance estimation (Hall et al., 1992), mineral exploration, and identification and radiation budget calculation (Prata et al., 1995). The satellite-based measurements can be modified via LSE in three ways:

i. The LSE reduces the top of atmosphere (ToA) radiance in comparison with a blackbody,
ii. Nonblack body surfaces reflecting downwelling radiances, and
iii. When we introduce the anisotropy of the LSE, it reduces or increases the surface leaving radiance.

The LSE can be calculated via Eq. (4):

$$LSE = \varepsilon s * (1 - FVC) + (\varepsilon v * FVC) \quad (4)$$

where εs = Emissivity of bare soil and εv = Emissivity of vegetation.

The surface temperature of the SCA (snow-covered area), sunlit and SCA shadow areas is determined via the TIRS band 10 data of Landsat-8, which are centered at 10.9 µm. Relative to band 10 data, band 11 data (centered at 12 µm) are affected by a greater stray light effect in the telescope, resulting in uncertainty in its calibration, which restricts its further use (Barsi, Lee, et al., 2014). To retrieve the surface temperature (Ts), initially, the spectral radiance at the sensor is converted to surface radiance, and then, Ts is calculated from the surface radiance values via Eq. (5).

$$LS = (Lsat - Lu) / \varepsilon\tau - (1 - \varepsilon)/ \varepsilon Ld \quad (5)$$

where LS = surface radiance after atmospheric correction, Lsat = spectral radiance at the sensor, Lu = upwelling spectral radiance between the surface and the sensor, ε = emissivity, τ = atmospheric transmission, and Ld = downwelling spectral radiance from the sky.

The corrected surface radiance values of band 10 are converted into surface temperatures via Eq. (6):

$$LST = \frac{K2}{In\left(\frac{K1}{LS}\right)+1} \quad (6)$$

where LTS = land surface temperature,
K1 and K2 = calibration constants, and
LS = surface radiance.

The LST is the radiative skin temperature of the land surface, as measured in the direction of the remote sensor. It is estimated from ToA brightness temperatures from the infrared spectral channels of a constellation of geostationary satellites. Its estimation further depends on the albedo, vegetation cover, and soil moisture.

UHIs and UTFVIs

The impact of UHIs has gained much attention in the field of urban climate and environmental change. Different methodologies have been employed globally to determine the extent and magnitude of UHIs (Faisal et al., 2021; Kim & Brown, 2021; Li et al., 2019). Advancements in remote sensing have made it possible to study UHIs via images. Additionally, LULC is linked to UHIs and the geographic distribution of vegetation intensity (Abubakar et al., 2024). The UHI effect is computed via Eq. (viii). On the other hand, the urban thermal variance field index (UTFVI) is the degree of thermal comfort that is calculated and used to determine the effect of UHIs on urban life quantitatively via Eqs. (7) and (8).

$$\text{UHI} = \frac{\text{LST}-\text{LSTmean}}{\text{STD}} \quad (7)$$

and

$$\text{UTFVI} = \frac{\text{TS}-\text{Tmean}}{TS} \quad (8)$$

where UTFVI is the urban thermal field variance index; TS is the LST of a pixel in °C; and Tmean is the mean LST of the study area in °C. The values of the UTFVI were divided into six tiers. Each categorization of the UTFVI is correlated with an ecological evaluation index (EEI). The ecological assessment index is a status indicator that qualitatively examines the influence of urban thermals on urban ecology (Zhang et al., 2006).

Vegetation Cooling Efficiency Index (VCEI)

This study proposed the vegetation cooling efficiency index (VCEI) to examine the influence of vegetation on LST. This is determined via Eq. (9).

$$LST = a + b * NDVI \quad (9)$$

The slope b b is the vegetation cooling efficiency index (VCEI). A negative slope indicates that vegetation cooled the surface, whereas values near zero or positive values of the slope indicate a poor cooling effect of vegetation. This could be in areas with sparse/dry vegetation, water bodies, and impervious surfaces.

RESULTS AND DISCUSSION

Accuracy assessment

Table 3 presents the accuracy assessment from the land use and land cover assessments for the years 2004, 2014, and 2024.

Table 3: Accuracy assessment of the 2004, 2014, and 2024 LULC classifications

	2004		2014		2024	
	Producer Accuracy	**User Accuracy**	**Producer Accuracy**	**User Accuracy**	**Producer Accuracy**	**User Accuracy**
Bare Land	88.54	90	93.5	95	88.58	90
Built-up	88.58	90	83.25	85	88.58	90
Cropland	84.25	88	88.58	90	78.7	80
Vegetation	73.8	75	75.23	78	70.2	70
Water	84.7	87	69.25	72	70.2	70
Overall Accuracy	86%		84%		80%	
Kappa Coefficient	0.919		0.891		0.888	

Source: Author's Analysis, 2024

For the 2004 land use/land cover classification, the overall accuracy was 0.86 (86%), which indicates a very high correlation, whereas the kappa coefficient was 0.919, which further established the level of accuracy of the observed land use pattern in Kaduna. For the 2014 land use/land cover classification, the overall accuracy was 0.84 (84%), which indicates a very high correlation between the classified and actual land cover types. The kappa coefficient is 0.891, which further establishes the level of accuracy of the observed land usage pattern in Kaduna.

The accuracy assessment of the 2024 land use and land cover classification is shown in Table 3. The overall accuracy is 0.80 (80%), which indicates a very high correlation between the classified and actual data. The kappa coefficient is 0.888, which further establishes the level of accuracy of the observed land usage pattern in Kaduna.

Land Use and Land Cover Changes

The magnitude of changes in each land use and land cover class was computed for the first epoch, which was between 2004 and 2014, and the second epoch, which was from 2014 to 2024. The results are shown in Table 4 and Figure. 2.

Table 4: Magnitude and rate of land use/land cover change in the Kaduna metropolis

Land Use	Magnitude of Change			Rate of Change		
	2004-2014	**2014-2024**	**2004-2024**	**2004-2014**	**2014-2024**	**2004-2024**
Bare	57.29	538.90	596.19	5.73	53.89	29.81
Built Area	26.05	94.99	121.04	2.61	9.50	6.05
Cultivated	-42.77	-482.77	-525.54	-4.28	-48.28	-26.28
Tree Cover	-40.78	-151.13	-191.91	-4.08	-15.11	-9.60
Water	0.21	0.02	0.22	0.02	0.00	0.01
Total	**0.00**	**0.00**	**0.00**			

Source: Author's Analysis, 2024

Table 4 reveals that between 2004 and 2014, bare land, built-up areas, and water bodies increased by 57.29 km^2, 26.06 km^2, and 0.21 km^2, respectively, whereas cultivated land and tree cover decreased by 42.77 km^2 and 40.78 km^2, respectively. Between 2014 and 2024, bare land, built-up areas, and water bodies increased by 538.90 km^2, 94.99 km^2, and 0.02 km^2, respectively, whereas cultivated land and tree cover lost 482.77 km^2 and 151.13 km^2, respectively. During the entire study period (2004--2024), bare land, built-up areas, and water bodies gained 596.19 km^2, 121.04 km^2, and 0.22 km^2, respectively, whereas cultivated land and tree cover lost 525.54 km^2 and 191.91 km^2, respectively. For the rate of land use land cover conversion in the Kaduna metropolis, Table 2 reveals that bare lands, built-up areas, and water bodies gained 5.73 km^2, 2.61 km^2, and 0.02 km^2, respectively, per annum, whereas cultivated lands and tree cover lost 4.28 km^2 and 4.08 km^2 per annum, respectively.

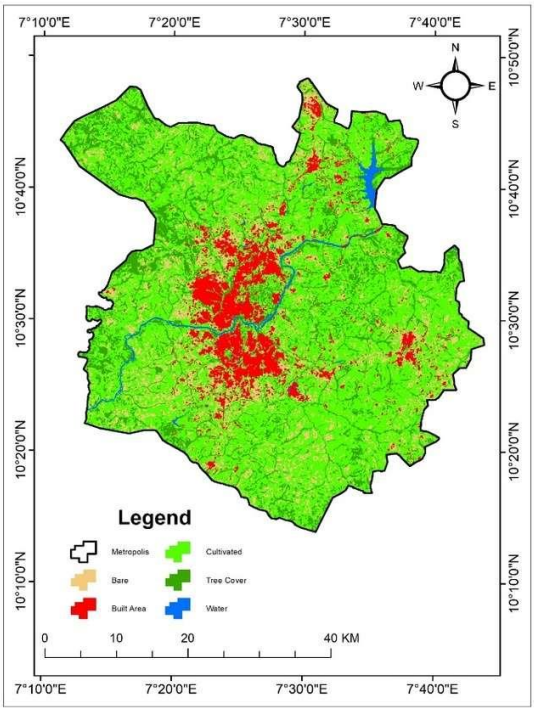

a) 2004

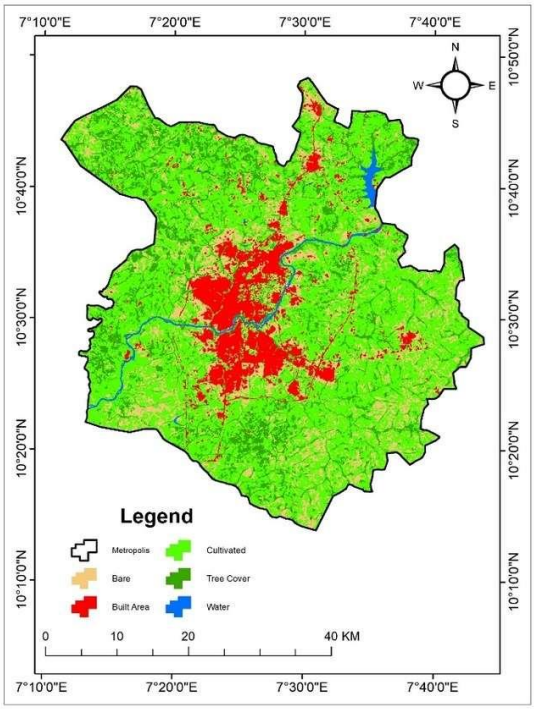

b) 2014

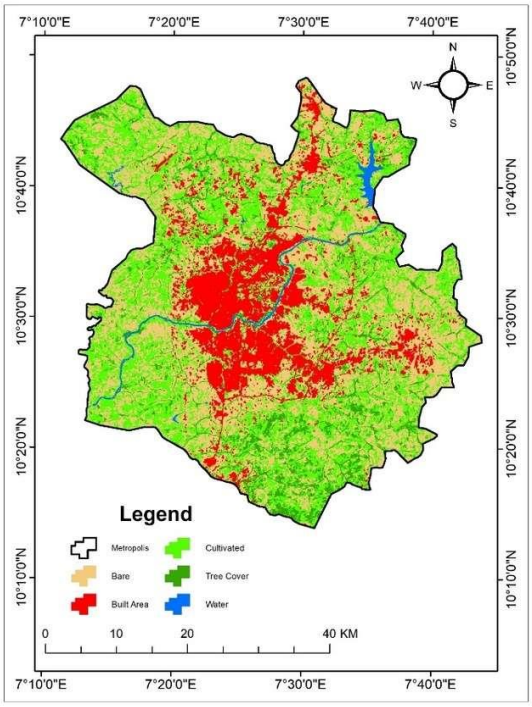

c) 2024

Figure 2: Land use/land cover characteristics of the Kaduna metropolis from 2004 to 2024

Spatiotemporal variation in LST

The results of the LST are shown in Table 5 and Figure 3.

Table 5: Distribution of land surface temperature in Kaduna from 2004-2024

Variables	LST		
	2004	**2014**	**2024**
Minimum	27.66	28.66	29.81
Maximum	36.26	37.19	39.69
Mean	32.16	33.18	35.67
STD	0.78	0.89	1.08

Table 5 shows the land surface temperature (LST) results for 2004, 2014, and 2024, revealing a clear warming trend over time, with both the minimum and maximum values, as well as the overall mean, steadily increasing. In 2004, the LST ranged between approximately 27.7 °C and 36.3 °C, with an average of 32.2 °C, but by 2014, these values had risen to a range of 28.7–37.2 °C and a mean of 33.2 °C, reflecting a moderate but consistent rise in surface heating. By 2024, the LST shows a sharper increase, with minimum values near 29.8 °C, maximum values approaching 39.7 °C, and an average of 35.7 °C—over 3.5 °C higher than two decades earlier. The gradual increase in standard deviation, from 0.78 in 2004 to 1.08 in 2024, further indicates a growing spatial variability in surface heating, suggesting intensifying heat extremes. Collectively, these results highlight both a progressive rise in baseline surface temperatures and widening disparities across the landscape, underscoring the influence of climate change and possible land use/land cover changes on local thermal environments.

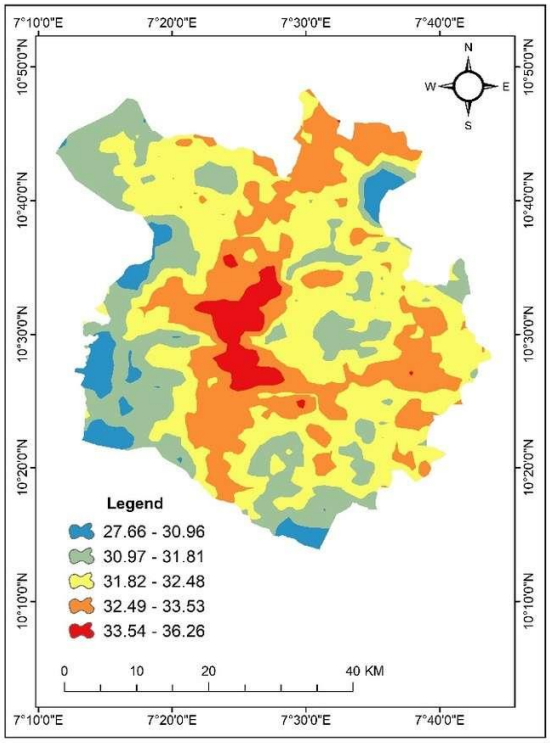

a) 2004

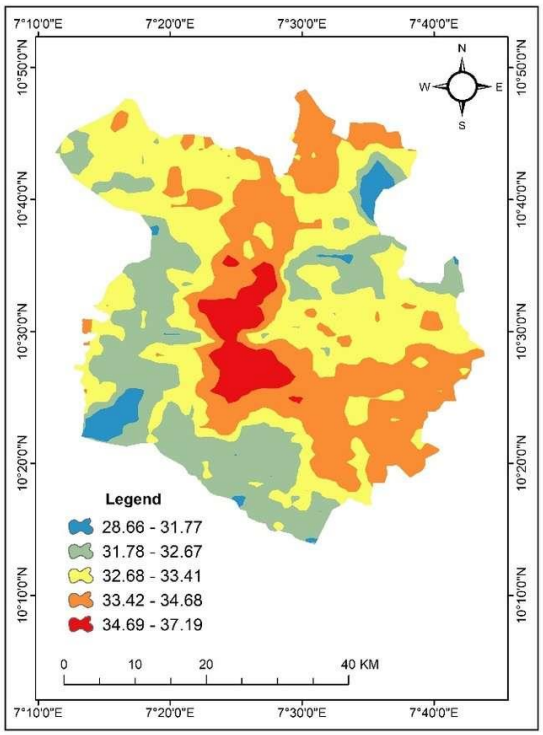

b) 2014

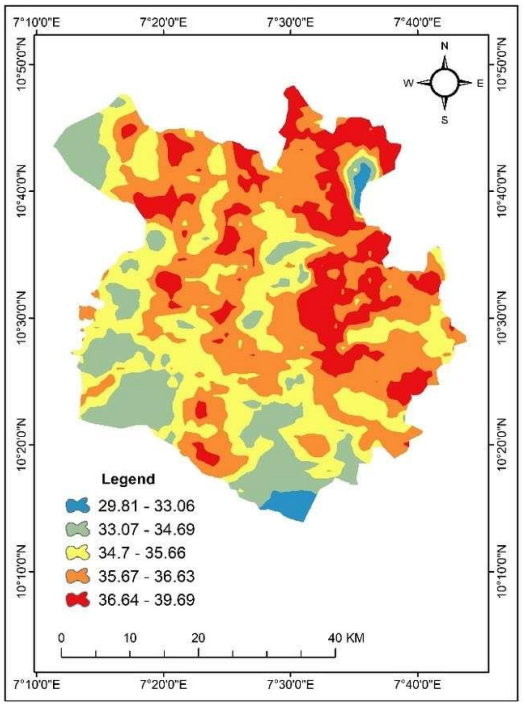

c) 2024

Figure 3: Land surface temperature of the Kaduna metropolis from 2004 to 2024

UHIs and UTFVIs

The temporal variations in the UHI effect and UTFVI are presented in this subsection. The results are shown in Table 6 and Figures 4 and 5.

Table 6: Spatiotemporal variation in the UHI effect

	2004	2014	2024
UHI			
Minimum	-5.80	-5.07	-5.43
Maximum	5.27	4.51	3.72
Mean	0.00	0.00	0.00
STD	1.00	1.00	1.00
UTFVI			
Minimum	-0.14	-0.14	-0.16
Maximum	0.13	0.12	0.11
Mean	0.00	0.00	0.00

Table 6 shows the urban heat island (UHI) results for 2004, 2014, and 2024, revealing a stable overall pattern, since the mean UHI across the study area remains at 0.00 for all three periods, an outcome of the normalization approach where deviations are measured relative to the mean land surface temperature (LST). However, the minimum and maximum values reveal important dynamics in the spatial variability of heat distribution. In 2004, the UHI intensity ranged from approximately –5.8 °C (areas cooler than the mean, likely vegetated or water-dominated surfaces) to +5.3 °C (areas significantly warmer than the mean, typically dense built-up zones). By 2014, the range had narrowed slightly (–5.07 °C to +4.51 °C), suggesting a mild reduction in thermal extremes, possibly linked to changes in land use or local climatic moderation. In 2024, the spread further contracted (–5.43 °C to +3.72 °C), indicating that while some areas are still cooler or hotter than average, the most intense hotspots are diminishing in magnitude. The constant standard deviation of 1.00 across years reflects that relative variability has been standardized, emphasizing comparative rather than absolute change. Overall, these results suggest that while UHIs persist, their peak intensity may weaken over time, potentially due to urban greening efforts, infrastructural changes, or broader increases in baseline temperatures, reducing the relative contrast between urban areas and surrounding rural areas.

The urban thermal field variance index (UTFVI) results for 2004, 2014, and 2024 demonstrate relatively small but meaningful variations in thermal stress across the study area. By definition, the mean remains at 0.00 for all years since the UTFVI expresses deviations in the LST relative to the area's average. The minimum values (–0.14 to –0.16) reflect areas that are consistently cooler than the mean, likely associated with vegetation, open land, or water bodies, whereas the maximum values (0.13 in 2004, declining slightly to 0.11 in 2024) correspond to localized urban or built-up hotspots. The gradual reduction in the maximum suggests that although urban areas continue to be warmer than their surroundings, the degree of thermal stress relative to the mean has weakened over time. Moreover, the increase in standard deviation from 0.02 in 2004 to 0.03 in 2014 and 2024 indicates slightly greater spatial variability in thermal conditions, meaning that while extremes are less intense, contrasts across the landscape are still becoming more scattered. Overall, the UTFVI findings suggest that ecological thermal stress remains moderate and fairly balanced, with no severe anomalies, but the persistence of both cooler and hotter zones underscores the importance of sustainable land use management to mitigate localized heat stress and maintain ecological resilience.

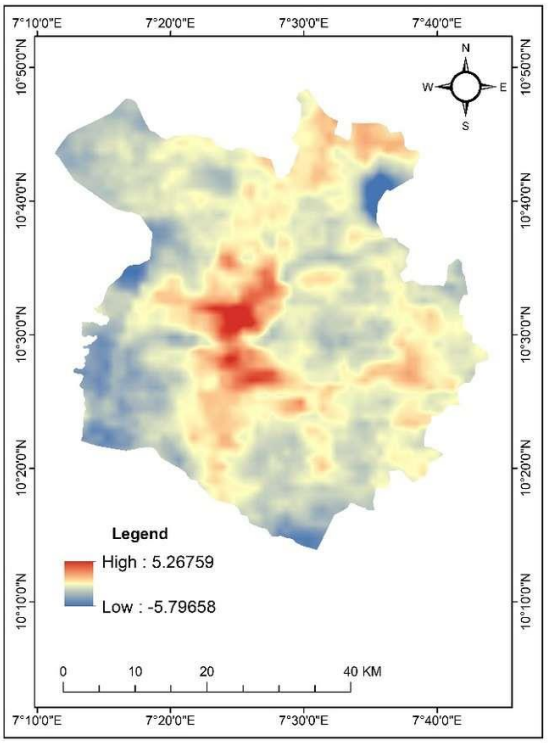

a) 2004

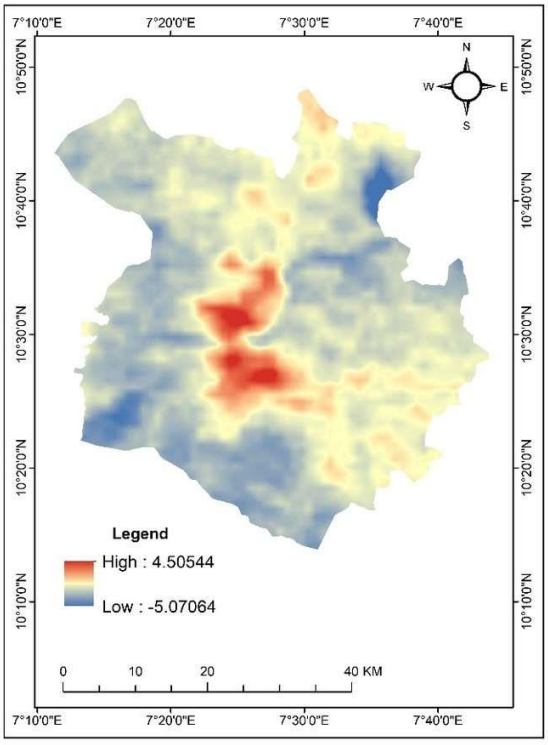

b) 2014

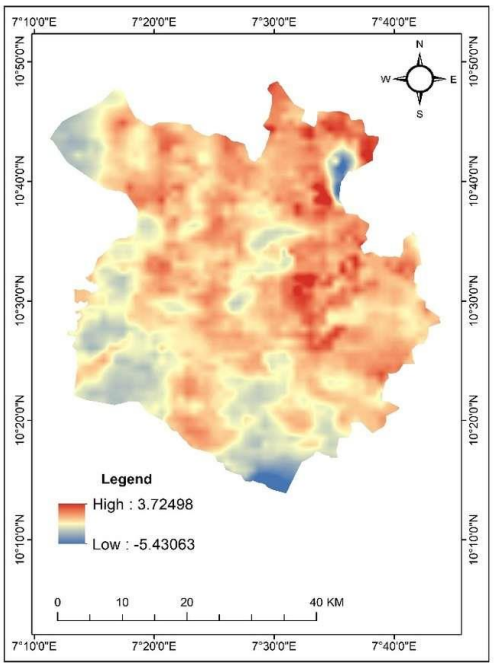

c) 2024

Figure 4: Urban heat islands of the Kaduna metropolis from 2004--2024

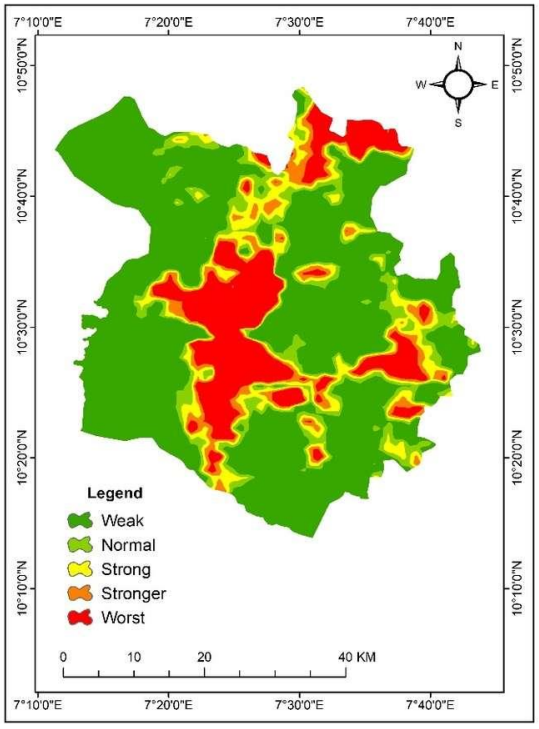

a) 2004

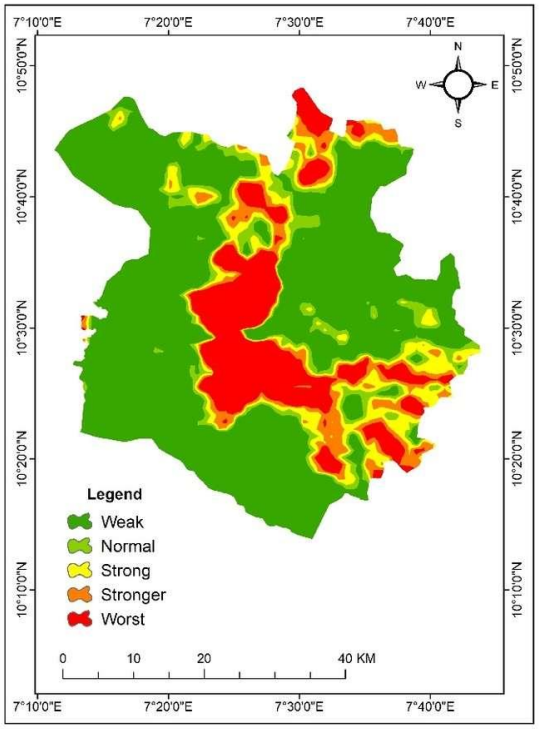

b) 2014

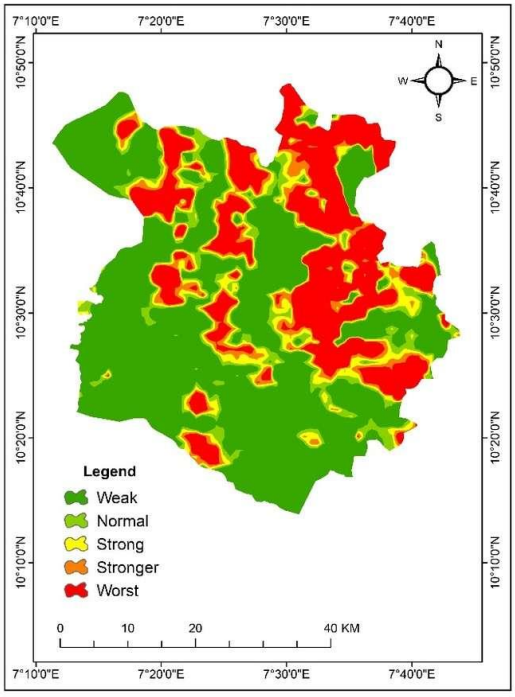

c) 2024

Figure 5: Urban thermal field variance index (UTFVI) of the Kaduna metropolis in 2004

VCEI

The vegetation cooling index was used to quantify the cooling influence of vegetation in the Kaduna metropolis. The results are shown in Table 7.

Table 7: Vegetation cooling efficiency index

	Slope	Intercept
Max	+1.39	43.5 °C
Mean	–16.90	39.7 °C
Min	–33.71	27.6 °C

Table 7 reveals that the calculated vegetation cooling efficiency index (VCEI) values ranged from –33.7 to +1.39, with a mean slope of –16.9. This implies that, on average, a unit increase in the NDVI corresponds to a reduction of ~17 °C in the land surface temperature. Areas with dense vegetation (NDVI > 0.6) presented the strongest cooling effect (–33 °C), whereas certain built-up/stressed vegetation zones presented negligible or even positive VCEI values (+1.3 °C). These results highlight the importance of vegetation in mitigating thermal discomfort while also emphasizing spatial heterogeneity in cooling efficiency across the landscape.

Discussions

This study examined the correlation between urban expansion and ecological thermal conditions in the Kaduna metropolis from 2004--2024, utilizing multitemporal Landsat data and indicators such as the LST, UHI, UTFVI, and the newly introduced vegetation cooling efficiency index (VCEI). These findings underscore that rapid urban expansion, marked by substantial expansions of developed regions and barren lands at the cost of agricultural land and forest cover, has significantly influenced surface temperature and ecological thermal comfort.

The spatiotemporal rise in the mean LST from 32.2 °C in 2004 to 35.7 °C in 2024 highlights the warming trend of the Kaduna metropolis, which aligns with observations from other African cities undergoing comparable urban transitions (Abd-Elmabod et al., 2022; Tesfamariam et al., 2024). The rise in impervious surfaces, the loss of plant cover, and the thermal characteristics of building materials all contributed to this increasing trend. These factors all lower evapotranspiration and increase surface heat storage. The higher standard deviation of the LST also shows that the temperature differences across the city are increasing, which exacerbates localized heat stress.

Research on UHIs has shown that built-up regions are consistently warmer than vegetated and water-dominated surfaces. This is similar to the findings of (Cetin et al., 2024) and (Siswanto et al., 2023), who revealed that urban surfaces such as concrete and asphalt absorb and retain more heat, while reducing vegetation limits cooling through evapotranspiration, and water bodies provide a cooling effect. The maximum UHI intensity decreased from +5.27 °C in 2004 to +3.72 °C in 2024, which shows that heat islands are still present, but their relative intensity has weakened over time. This study contradicts the typical assumption of increasing UHI severity in rapidly urbanizing areas. A probable reason is the general rise in baseline temperatures across the city, which narrows the relative difference between urban and peri-urban zones. The Kaduna Urban Renewal Programme (Kaduna State Government, 2021) is also making improvements to infrastructure and adding more green space, which may have helped cool some of the hottest places.

The UTFVI data revealed modest ecological stress, with both cooler (vegetated) and warmer (built-up) zones remaining

throughout the study period. The gradual decrease in the maximum UTFVI values suggests fewer temperature extremes, whereas the increase in standard deviation indicates greater heterogeneity in thermal comfort across the metropolis. This result is similar to the findings of (Mokarram et al., 2023), who reported that a decline in UTFVI values suggests worsening ecological comfort due to urbanization and reduced vegetation. This regional heterogeneity means that while overall ecological circumstances remain generally balanced, small pockets of discomfort continue and could grow under future climate change.

The proposed VCEI further highlights the crucial role of vegetation in regulating surface temperature. The negative slope results confirmed that vegetation has a cooling impact across the Kaduna metropolis; however, the effects differ in terms of efficiency depending on vegetation density and health. The lowering of this cooling efficacy in areas of sparse or damaged vegetation is consistent with findings from earlier studies emphasizing the sensitivity of urban greenery to rapid land change (Litardo et al., 2020; Patel et al., 2024). This highlights the necessity of conserving and growing urban green infrastructure to sustain the cooling advantages of vegetation.

Taken together, the results reveal that uncontrolled urban expansion in the Kaduna metropolis has produced major thermal modifications, with implications for human health, energy demand, and urban ecology. If uncontrolled, these dynamics could worsen urban heat stress and jeopardize progress toward the Sustainable Development Goals (SDGs), particularly SDG 11 (sustainable cities and communities) and SDG 13 (climate action).

CONCLUSION

This study investigated the impacts of urban expansion on ecological thermal comfort in the Kaduna metropolis over two decades via Landsat imagery and indices such as the LST, UHI, UTFVI, and proposed VCEI. The results demonstrated a significant change in agricultural land and tree cover into built-up areas and barren lands, resulting in a constant increase in land surface temperature and mild but persistent ecological stress. Although the intensities of the UHI and UTFVI marginally diminished over time, the persistence of thermal hotspots demonstrates the vulnerability of urban populations to localized heat stress. The VCEI validated the critical cooling effect of vegetation, although its efficacy is being degraded by continuing land change. The study revealed that increasing urbanization in the Kaduna metropolis is altering the city's ecological balance and thermal environment. To increase resilience and improve thermal comfort, policymakers and planners should emphasize policies that retain and expand vegetation cover, incorporate green infrastructure into new constructions, and use climate-sensitive designs in urban regeneration programs. Protecting vegetation is particularly crucial, as it remains the most effective natural buffer against rising surface temperatures. Future research should incorporate household-level exposure evaluations, socioeconomic vulnerability analysis, and predictive climate models to provide more holistic knowledge of urban thermal dynamics and adaptation routes for Kaduna and similar cities in sub-Saharan Africa.

Data availability statement

The datasets generated during and/or analysed during the current study are available from the corresponding author on reasonable request.

REFERENCES

Abd-Elmabod, S. K., Jiménez-González, M. A., Jordán, A., Zhang, Z., Mohamed, E. S., Hammam, A. A., El Baroudy, A. A., Abdel-Fattah, M. K., Abdelfattah, M. A., & Jones, L. (2022). Past and future impacts of urbanisation on land surface temperature in Greater Cairo over a 45 year period. *The Egyptian Journal of Remote Sensing and Space Science*, *25*(4), 961–974. https://doi.org/10.1016/j.ejrs.2022.10.001

Abdussalam, A. F. (2020). Climate Change and Health Vulnerability in Informal Urban Settlements of Kaduna Metropolis. *Science World Journal*, *15*(3), 127–132. https://doi.org/10.47514/swj/15.03.2020.020

Abubakar, M. L. (2019). Analysis of Land Use Land Cover in Danja Local Government Area, Katsina - Nigeria, From 1986 To 2019. *60th Annual Conference of the Association of Nigerian Geographers (ANG)*. https://doi.org/10.13140/RG.2.2.12948.65920

Abubakar, M. L., & Abdussalam, A. F. (2024). Geospatial analysis of land use changes and wetland dynamics in Kaduna Metropolis, Kaduna, Nigeria. *Science World Journal*, *19*(3), 687–696. https://doi.org/10.4314/swj.v19i3.15

Abubakar, M. L., Thomas, D., Ahmed, M. S., & Abdussalam, A. F. (2024). Assessment of the Relationship Between Land Surface Temperature and Vegetation Using MODIS LST and NDVI Timerseries Data in Kaduna Metropolis, Nigeria. *FUDMA JOURNAL OF SCIENCES*, *8*(2), 137–148. https://doi.org/10.33003/fjs-2024-0802-2305

Adão, F., Fraga, H., Fonseca, A., Malheiro, A. C., & Santos, J. A. (2023). The Relationship between Land Surface Temperature and Air Temperature in the Douro Demarcated Region, Portugal. *Remote Sensing 2023, Vol. 15, Page 5373*, *15*(22), 5373. https://doi.org/10.3390/RS15225373

Agarwal, C., & Sharma, A. (2011). Image understanding using decision tree based machine learning. *2011 International Conference on Information Technology and Multimedia: "Ubiquitous ICT for Sustainable and Green Living", ICIM 2011*. https://doi.org/10.1109/ICIMU.2011.6122757

Ahmed, M. S., Abubakar, M. L., Lawal, A. I., & Richifa, K. I. (2024). Influence of extreme temperature on adverse pregnancy outcomes in Kaduna State, Nigeria. *Science World Journal*, *19*(2), 409–417. https://doi.org/10.4314/swj.v19i2.17

Ajibade, L. T., & Okwori, A. (2009). Developing an Information System for Rural Water Supply Scheme in Kaduna State. *Journal of Environmental Science*, *1*(1), 1–8.

Akpu, B., Tanko, A., Jeb, D., & Dogo, B. (2017). Geospatial Analysis of Urban Expansion and Its Impact on Vegetation Cover in Kaduna Metropolis, Nigeria. *Asian Journal of Environment & Ecology*, *3*(2), 1–11. https://doi.org/10.9734/ajee/2017/31149

Al Shawabkeh, R., AlHaddad, M., Al-Fugara, A., Al-Hawwari, L., Al-Hawwari, M. I., Omoush, A., & Arar, M. (2023). Modeling the impact of urban land cover features and changes on the land surface temperature (LST): The case of Jordan. *Ain Shams Engineering Journal*, *June*, 102359. https://doi.org/10.1016/j.asej.2023.102359

Alawamy, J. S., Balasundram, S. K., Mohd. Hanif, A. H., & Boon Sung, C. T. (2020). Detecting and Analyzing Land Use and Land Cover Changes in the Region of Al-Jabal Al-Akhdar, Libya Using Time-Series Landsat Data from 1985 to 2017. *Sustainability*, *12*(11), 4490. https://doi.org/10.3390/su12114490

Amin, M., & Dadan-Garba, A. (2014). Urban Vegetation Study of Kaduna Metropolis using GIS and Remotely sensed Data. *Journal of Natural Sciences Research*, *4*(4), 160–171.

Andronis, V., Karathanassi, V., Tsalapati, V., Kolokoussis, P., Miltiadou, M., & Danezis, C. (2022). Time Series Analysis of Landsat Data for Investigating the Relationship between Land Surface Temperature and Forest Changes in Paphos Forest, Cyprus. *Remote Sensing*, *14*(1010). https://doi.org/10.3390/rs14041010

Arias, M., Notarnicola, C., Campo-Bescós, M. Á., Arregui, L. M., & Álvarez-Mozos, J. (2023). Evaluation of soil moisture estimation techniques based on Sentinel-1 observations over wheat fields. *Agricultural Water Management*, *287*, 108422. https://doi.org/10.1016/J.AGWAT.2023.108422

Avdan, U., & Jovanovska, G. (2016). Algorithm for Automated Mapping of Land Surface Temperature Using LANDSAT 8 Satellite Data. *Journal of Sensors*, *2016*, 1–8. https://doi.org/10.1155/2016/1480307

Baba, B. M., Abubakar, M. L., Raji, R. B., & Ibrahim, R. (2020). Spatial Distribution of Electric Transformers in Narayi Ward, Chikun Local Government Area of Kaduna State, Nigeria. *Kaduna Journal of Geography*, *2*(2), 114–130. https://doi.org/10.5281/zenodo.14598765

Barsi, J. A., Lee, K., Kvaran, G., Markham, B. L., & Pedelty, J. A. (2014). The spectral response of the Landsat-8 operational land imager. *Remote Sensing*, *6*(10), 10232–10251. https://doi.org/10.3390/rs61010232

Barsi, J. A., Schott, J., Hook, S., Raqueno, N., Markham, B., & Radocinski, R. (2014). Landsat-8 Thermal Infrared Sensor (TIRS) Vicarious Radiometric Calibration. *Remote Sensing*, *6*(11), 11607–11626. https://doi.org/10.3390/rs61111607

Basu, A., & Das, S. (2021). *Afforestation, revegetation, and regeneration: a case study on Purulia district, West Bengal (India)* (pp. 497–524). https://doi.org/10.1016/B978-0-12-823895-0.00014-2

Becker, F. (1987). The impact of spectral emissivity on the measurement of land surface temperature from a satellite. *International Journal of Remote Sensing*, *8*(10), 1509–1522. https://doi.org/10.1080/01431168708954793

Bennett, J. G., Rains, A. B., Gosden, P. N., Howard, W. J., Hutcheon, A. A., Kerr, W. B., Mansfield, J. E., Rackham, L. J., & Wood, A. W. (1979). Land Resources of central Nigeria; agricultural development possibilities. Volume 3A. The Jema'a Platform Executive Summary. In I. D. Hill (Ed.), *Agricultural development possibilities: The Jema'a Platform* (Vol. 3B). Land Resources Development Centre.

Bharath, H. A., Nimish, G., & Chandan, M. C. (2020). Exposition of spatial urban growth pattern using PSO-SLEUTH and identifying its effects on surface temperature. In *Urban Ecology* (pp. 49–68). Elsevier. https://doi.org/10.1016/B978-0-12-820730-7.00004-5

Cetin, M., Ozenen Kavlak, M., Senyel Kurkcuoglu, M. A., Bilge Ozturk, G., Cabuk, S. N., & Cabuk, A. (2024). Determination of land surface temperature and urban heat island effects with remote sensing capabilities: the case of Kayseri, Türkiye. *Natural Hazards*, *120*(6), 5509–5536. https://doi.org/10.1007/S11069-024-06431-5/METRICS

Congalton, R. G. (1991). A review of assessing the accuracy of classifications of remotely sensed data. *Remote Sensing of Environment*, *37*(1), 35–46. https://doi.org/10.1016/0034-4257(91)90048-B

Das, D. N., Chakraborti, S., Saha, G., Banerjee, A., & Singh, D. (2020). Analysing the dynamic relationship of land surface temperature and landuse pattern: A city level analysis of two climatic regions in India. *City and Environment Interactions*, *8*, 100046. https://doi.org/10.1016/j.cacint.2020.100046

Faisal, A. Al, Kafy, A. A., Al Rakib, A., Akter, K. S., Jahir, D. M. A., Sikdar, M. S., Ashrafi, T. J., Mallik, S., & Rahman, M. M. (2021). Assessing and predicting land use/land cover, land surface temperature and urban thermal field variance index using Landsat imagery for Dhaka Metropolitan area. *Environmental Challenges*, *4*. https://doi.org/10.1016/J.ENVC.2021.100192

GRID3 - Nigeria. (2024). *Geo-Referenced Infrastructure and Demographic Data for Development*. National Space Research and Development Agency. http://grid3.gov.ng/

Hidalgo-García, D., & Arco-Díaz, J. (2022). Modeling the Surface Urban Heat Island (SUHI) to study of its relationship with variations in the thermal field and with the indices of land use in the metropolitan area of Granada (Spain). *Sustainable Cities and Society*, *87*(March). https://doi.org/10.1016/j.scs.2022.104166

Kaduna Bureau of Statistics. (2015). *Population Projections for Kaduna State*.

Kaduna State Government. (2021). *El-Rufai launches Kaduna Urban Renewal Project*.

Kim, S. W., & Brown, R. D. (2021). Urban heat island (UHI) intensity and magnitude estimations: A systematic literature review. *Science of The Total Environment*, *779*, 146389. https://doi.org/10.1016/j.scitotenv.2021.146389

Kodors, S. (2019). Detection of Man-Made Constructions Using LiDAR Data and Decision Trees. *Baltic Journal of Modern Computing*, *7*(2). https://doi.org/10.22364/bjmc.2019.7.2.05

Koko, A. F., Wu, Y., Abubakar, G. A., Alabsi, A. A. N., Hamed, R., & Bello, M. (2021). Thirty Years of Land Use/Land Cover Changes and Their Impact on Urban Climate: A Study of Kano Metropolis, Nigeria. *Land*, *10*(11), 1106. https://doi.org/10.3390/LAND10111106

Koko, A. F., Yue, W., Abubakar, G. A., Alabsi, A. A. N., & Hamed, R. (2021). Spatiotemporal influence of land use/land cover change dynamics on surface urban heat island: A case study of abuja metropolis, nigeria. *ISPRS International*

Journal of Geo-Information, *10*(5). https://doi.org/10.3390/ijgi10050272

Kusumawardani, K. P., & Hidayati, I. N. (2022). Analysis of urban heat island and urban ecological quality based on remote sensing imagery transformation in semarang city. *IOP Conference Series: Earth and Environmental Science*, *1089*(1). https://doi.org/10.1088/1755-1315/1089/1/012037

Laliberte, A. S., Fredrickson, E. L., & Rango, A. (2007). Combining decision trees with hierarchical object-oriented image analysis for mapping arid rangelands. *Photogrammetric Engineering and Remote Sensing*, *73*(2), 197–207. https://doi.org/10.14358/PERS.73.2.197

Li, X., Zhou, Y., Yu, S., Jia, G., Li, H., & Li, W. (2019). Urban heat island impacts on building energy consumption: A review of approaches and findings. *Energy*, *174*, 407–419. https://doi.org/10.1016/j.energy.2019.02.183

Litardo, J., Palme, M., Borbor-Cordova, M., Caiza, R., Macias, J., Hidalgo-Leon, R., & Soriano, G. (2020). Urban Heat Island intensity and buildings' energy needs in Duran, Ecuador: Simulation studies and proposal of mitigation strategies. *Sustainable Cities and Society*, *62*(July), 102387. https://doi.org/10.1016/j.scs.2020.102387

Mahato, S., Kundu, B., Makwana, N., & Joshi, P. K. (2023). Early summer temperature anomalies and potential impacts on achieving Sustainable Development Goals (SDGs) in National Capital Region (NCR) of India. *Urban Climate*, *52*, 101705. https://doi.org/10.1016/j.uclim.2023.101705

Mhana, K. H., Norhisham, S. Bin, Katman, H. Y. B., & Yaseen, Z. M. (2023). Environmental impact assessment of transportation and land alteration using Earth observational datasets: Comparative study between cities in Asia and Europe. *Heliyon*, *9*(9), e19413. https://doi.org/10.1016/j.heliyon.2023.e19413

Moisa, M. B., & Gemeda, D. O. (2022). Assessment of urban thermal field variance index and thermal comfort level of Addis Ababa metropolitan city, Ethiopia. *Heliyon*, *8*(8). https://doi.org/10.1016/j.heliyon.2022.e10185

Mokarram, M., Taripanah, F., & Pham, T. M. (2023). Investigating the effect of surface urban heat island on the trend of temperature changes. *Advances in Space Research*, *72*(8), 3150–3169. https://doi.org/10.1016/j.asr.2023.06.048

Muhammad, R. Z., & Abubakar, M. L. (2025). Assessing the influence of land surface temperature and sociodemographic factors on measles prevalence using AutoML and SHAP in Kaduna North, Nigeria. *GeoJournal*, *90*(3), 103. https://doi.org/10.1007/s10708-025-11361-1

Musa, K., & Abubakar, M. L. (2024). Monitoring urban growth and landscape fragmentation in Kaduna, Nigeria, using remote sensing approach. *Journal of Degraded and Mining Lands Management*, *12*(1), 6757–6769. https://doi.org/10.15243/jdmlm.2024.121.6757

Naserikia, M., Hart, M. A., Nazarian, N., Bechtel, B., Lipson, M., & Nice, K. A. (2023). Land surface and air temperature dynamics: The role of urban form and seasonality. *Science of The Total Environment*, *905*, 167306. https://doi.org/10.1016/J.SCITOTENV.2023.167306

Norman, J. M., & Becker, F. (1995). Terminology in thermal infrared remote sensing of natural surfaces. *Agricultural and Forest Meteorology*, *77*(3–4), 153–166. https://doi.org/10.1016/0168-1923(95)02259-Z

Patel, S., Indraganti, M., & Jawarneh, R. N. (2024). Urban planning impact on summer human thermal comfort in Doha, Qatar. *Building and Environment*, *254*(February), 111374. https://doi.org/10.1016/j.buildenv.2024.111374

Peacock, R. (2014). *Accuracy Assessment of Supervised and Unsupervised Classification Using Landsat Imagery of Little Rock, Arkansas*. NORTHWEST MISSOURI STATE UNIVERISTY.

Peng, X., Wu, W., Zheng, Y., Sun, J., Hu, T., & Wang, P. (2020). Correlation analysis of land surface temperature and topographic elements in Hangzhou, China. *Scientific Reports*, *10*(1), 1–16. https://doi.org/10.1038/s41598-020-67423-6

Phiri, D., Simwanda, M., Nyirenda, V., Murayama, Y., & Ranagalage, M. (2020). Decision Tree Algorithms for Developing Rulesets for Object-Based Land Cover Classification. *ISPRS International Journal of Geo-Information*, *9*(5), 329. https://doi.org/10.3390/ijgi9050329

Prata, A. J., V. Casellescoll, C., Sobrino, J. A., & Ottle, C. (1995). Thermal remote sensing of land surface temperature from satellites: current status and future prospects. *Remote Sensing Reviews*, *12*(3–4), 175–224. https://doi.org/10.1080/02757259509532285

Rao, P., Tassinari, P., & Torreggiani, D. (2023). Exploring the land-use urban heat island nexus under climate change conditions using machine learning approach: A spatio-temporal analysis of remotely sensed data. *Heliyon*, *9*(8), e18423. https://doi.org/10.1016/j.heliyon.2023.e18423

Rashid, N., Alam, J. A. M. M., Chowdhury, M. A., & Islam, S. L. U. (2022). Impact of landuse change and urbanization on urban heat island effect in Narayanganj city, Bangladesh: A remote sensing-based estimation. *Environmental Challenges*, *8*(June), 100571. https://doi.org/10.1016/j.envc.2022.100571

Rousta, I., Sarif, M. O., Gupta, R. D., Olafsson, H., Ranagalage, M., Murayama, Y., Zhang, H., & Mushore, T. D. (2018). Spatiotemporal analysis of land use/land cover and its effects on surface urban heat Island using landsat data: A case study of Metropolitan City Tehran (1988-2018). *Sustainability (Switzerland)*, *10*(12). https://doi.org/10.3390/su10124433

Rwanga, S. S., & Ndambuki, J. M. (2017). Accuracy Assessment of Land Use/Land Cover Classification Using Remote Sensing and GIS. *International Journal of Geosciences*, *08*(04), 611–622. https://doi.org/10.4236/ijg.2017.84033

Sandoval, S., Escobar-Flores, J. G., & Badar Munir, M. (2023). Urbanization and its impacts on land surface temperature and sea surface temperature in a tourist region in Mexico from 1990 to 2020. *Remote Sensing Applications: Society and Environment*, *32*(July), 101046. https://doi.org/10.1016/j.rsase.2023.101046

Sharma, A., & Vashishtha, D. (2023). Spatio-temporal Assessment of Land Use Land Cover Changes and Their Impact on Variations of Land Surface Temperature in Aligarh Municipality. *Journal of the Indian Society of Remote Sensing*, *51*(4), 799–827. https://doi.org/10.1007/s12524-022-01652-2

Shukla, A., & Jain, K. (2021). Analyzing the impact of changing landscape pattern and dynamics on land surface temperature in Lucknow city, India. *Urban Forestry and Urban Greening*, *58*, 126877. https://doi.org/10.1016/j.ufug.2020.126877

Siddique, M. A., Boqing, F., & Dongyun, L. (2023). Modeling the Impact and Risk Assessment of Urbanization on Urban Heat Island and Thermal Comfort Level of Beijing City, China (2005–2020). *Sustainability*, *15*(7), 1–18.

Singh, M. S., Kumar, D. P., Parijat, D. R., Gonengcil, B., & Rai, M. A. (2023). Establishing the relationship between land use land cover, normalized difference vegetation index and land surface temperature: A case of Lower Son River Basin, India. *Geography and Sustainability*. https://doi.org/10.1016/J.GEOSUS.2023.11.006

Siswanto, S., Nuryanto, D. E., Ferdiansyah, M. R., Prastiwi, A. D., Dewi, O. C., Gamal, A., & Dimyati, M. (2023). Spatio-temporal characteristics of urban heat Island of Jakarta metropolitan. *Remote Sensing Applications: Society and Environment*, *32*(September), 101062. https://doi.org/10.1016/j.rsase.2023.101062

Statista. (2024). *Nigeria: Urbanization from 2012 to 2022*.

Sugianto, S., Arabia, T., Rusdi, M., Syakur, S., & Trishiani, M. (2023). Spatial distribution vegetation density, land surface temperature, and land surface moisture of Banda Aceh, Indonesia after 17 years of tsunami: a multitemporal analysis approaches. *Environmental Monitoring and Assessment*, *195*(1), 1–23. https://doi.org/10.1007/S10661-022-10827-W/METRICS

Taripanah, F., & Ranjbar, A. (2021). Quantitative analysis of spatial distribution of land surface temperature (LST) in relation Ecohydrological, terrain and socio- economic factors based on Landsat data in mountainous area. *Advances in Space Research*, *68*(9), 3622–3640. https://doi.org/10.1016/j.asr.2021.07.008

Tesfamariam, S., Govindu, V., & Uncha, A. (2023). Spatio-temporal analysis of urban heat island (UHI) and its effect on urban ecology: The case of Mekelle city, Northern Ethiopia. *Heliyon*, *9*(2), e13098. https://doi.org/10.1016/J.HELIYON.2023.E13098

Tesfamariam, S., Govindu, V., & Uncha, A. (2024). Urban ecology in the context of urban heat island vulnerability potential zone mapping: the case of Mekelle city, Ethiopia. *Frontiers in Climate*, *6*(December). https://doi.org/10.3389/fclim.2024.1446048

Ullah, W., Ahmad, K., Ullah, S., Ahmad, A., Faisal, M., Nazir, A., Mehmood, A., Aziz, M., & Mohamed, A. (2023). Analysis of the relationship among land surface temperature (LST), land use land cover (LULC), and normalized difference vegetation index (NDVI) with topographic elements in the lower Himalayan region. *Heliyon*, *9*(2), e13322. https://doi.org/10.1016/j.heliyon.2023.e13322

Ünsal, Ö., Lotfata, A., & Avcı, S. (2023). Exploring the Relationships between Land Surface Temperature and Its Influencing Determinants Using Local Spatial Modeling. *Sustainability (Switzerland)*, *15*(15). https://doi.org/10.3390/su151511594

Wemegah, C. S., Yamba, E. I., Aryee, J. N. A., Sam, F., & Amekudzi, L. K. (2020). Assessment of urban heat island warming in the greater accra region. *Scientific African*, *8*, e00426. https://doi.org/10.1016/j.sciaf.2020.e00426

World Bank. (2023). *Urban population (% of total population) - Nigeria*. United Nations Population Division. World Urbanization Prospects: 2018 Revision.

Zaharaddeen, I., Baba, I. I., & Ayuba, Z. (2016). Estimation of land surface temperature of Kaduna Metropolis, Nigeria using landsat images. *Science World Journal*, *11*(3), 36–42.

Zandi, R., Zanganeh, Y., Karami, M., & Khosravian, M. (2022). Analysis of the Spatio-temporal variations of thermal patterns of Shiraz city by satellite images and GIS processing. *Egyptian Journal of Remote Sensing and Space Science*, *25*(4), 1069–1088. https://doi.org/10.1016/j.ejrs.2022.11.005

Zhang, Y., Yu, T., & Gu, X. (2006). Land surface temperature retrieval from CBERS-02 IRMSS thermal infrared data and its applications in quantitative analysis of urban heat island effect. *National Remote Sensing Bulletin*, *10*(5), 789–797. https://doi.org/10.1016/S0379-4172(06)60102-9